Journal of Applied Polymer Science

Properties and Phase Segregation of Crosslinked PCL-Based Polyurethanes

Aysun Güney,[1,2,3] Nesrin Hasirci[1,2,3,4]

[1]Department of Chemistry, Faculty of Arts and Sciences, Middle East Technical University, Ankara 06800, Turkey
[2]Graduate Department of Polymer Science and Technology, Middle East Technical University, Ankara 06800, Turkey
[3]BIOMATEN-Center of Excellence in Biomaterials and Tissue Engineering, Middle East Technical University, Ankara 06800, Turkey
[4]Graduate Department of Biotechnology, Middle East Technical University, Ankara 06800, Turkey
Correspondence to: N. Hasirci (E-mail: nhasirci@metu.edu.tr).

ABSTRACT: Polyurethane (PU) films were prepared from different types of poly(ε-caprolactone) glycols and hexamethylene diisocyanate without using any other ingredients such as solvent, catalyst, or chain extender. Polymers were stabilized by crosslinking formed as allophanate and/or biuret linkages during the curing process. The effects of different components on the product properties such as chemical structure, microphase segregation, mechanical strength, thermo-mechanical, thermal properties, and surface hydrophilicities were investigated by FTIR-ATR, atomic force microscope, mechanical tester, dynamic mechanical analyses, thermogravimetric analyzer, differential scanning calorimetry, and contact angle measurements. Phase separation of hard and soft segments significantly varied depending on the type and molecular weight of diol and triol. Films containing urethane-urea bonds displayed the maximum phase separation and the highest mechanical strength. Polyols having higher molecular weight increased hydrophilicity while urea bonds caused a reverse effect resulted by bidentate hydrogen bonds. Results showed PUs with various properties can be synthesized via environmentally friendly process without using any solvent or catalyst. © 2013 Wiley Periodicals, Inc. J. Appl. Polym. Sci. **2014**, *131*, 39758.

KEYWORDS: structure–property relations; polyurethanes; phase behavior; crosslinking

Received 22 January 2013; accepted 14 July 2013
DOI: 10.1002/app.39758

INTRODUCTION

Controllable properties of polyurethanes (PUs) make them attractive for various applications. PU products having different properties varying from elastic to viscous, from soft to hard, and from fiber to porous can be obtained by changing the preparation parameters.[1–5] Elastic and biodegradable PUs have found widespread applications as soft and hard tissue supports in medical studies, such as vascular smooth muscle,[6] cardiac muscle,[7] blood vessel,[8] skeletal muscle,[9] tendon,[10] ligament,[11] skin repair,[12] cartilage,[13,14] and bone.[15,16] According to the application area, they can be easily modified to be antithrombogenic,[17] antibacterial,[18] biocompatible,[19] and hydrophilic materials.[4,20] Because of their inherent hemocompatibility, they are also applicable in blood contacting devices such as heart valves, artificial veins, and catheters.[21,22]

PUs have domains such as hard segments (HS) and soft segments (SS) in their structures, where the amount and the distribution of these segments play an important role in determining the properties of the final product. HS is generally ordered domain having urethane linkages, and SS is amorphous part consisting macro-glycol moieties. In general, HS is randomly dispersed in SS continuous matrix. A third phase of crystalline SS can be observed in some PU structures. The segregation of micron size phases is the result of thermodynamic incompatibility of polar HS and less polar SS domains.[23,24] Organization of HS domains and inter- and intra-interactions between them determine interconnectivity influencing the extent of phase separation in the final urethane matrix. Also, both microphase segregation and existence of hydrogen bonding in HS domains cause formation of highly ordered structures in these segments. Higher phase separation and stronger hydrogen bonding in HS-HS results in improved thermal and mechanical properties.[25–27] Degree of phase separation depends on the chemical structure and fractions of the initial components, molecular weights and polydispersity of the SS components, thermal history of the polymers, and processing parameters.[28,29]

PU synthesis generally was done by mixing of a diisocyanate compound with a polyol and a chain extender in the existence

of solvent and catalyst.[30] Addition of excess diisocyanate is widely used for covalent crosslinking and provides shape recovery ability which does not exist in linear PU structures.[31] Organic solvents, crosslinkers, or other ingredients which are used in the polymer synthesis may cause some toxic effects and should have to be removed from the final product. Purification steps generally need rigorous conditions with extra energy consumption.[32–34] Therefore, in the last decades, environmentally friendly productions without using solvents or ingredients received a great attention. In PU synthesis, physical or chemical crosslinks can be generated by secondary reactions (such as allophanate and biuret formation) of the urethane linkages. In literature, it was reported that, synthesis of poly(ε-caprolactone) diol (PCL-diol) based PUs was done in a nonsolvent media by using 1,4-butanediol chain extender. It was given that either two phases (crystalline HS dissolved in amorphous SS) or three phases (additional crystalline PCL phase) were observed depending on the molecular weight of PCL.[35] Ping et al. reported that PUs produced from symmetrical isocyanates such as 1,6-hexamethylene diisocyanate (HDI) and diphenylmethane diisocyanate had higher degree of microphase separation due to better crystallization in HS domains compared with the ones produced from toluene diisocyanate and isophorone diisocyanate.[36] Bil et al. synthesized PUs by using PCL-diol with different molar masses and isocyanates with different amounts (HS content in the range of 22–70 wt %), and reported that as the concentrations of HS increased, the obtained PUs exhibited more phase separation and higher hydrophilicity.[37]

In this study, PCL-based PUs were prepared in medical purity, by using only glycol and isocyanate components without using any other ingredient such as solvent, catalyst, or chain extender. For this purpose, different glycols such as PCL-diol or poly(ε-caprolactone) triol (PCL-triol) were used with HDI. To the best of our knowledge, there is no report in literature addressing the structure–property relationship of crosslinked PUs synthesized with this technique in medical purity. In this study, the effects of initial composition and preparation conditions on phase separation as well as thermal and mechanical properties and hydrophilicity of the prepared PUs are discussed in detailed.

MATERIALS AND METHODS

Materials

HDI was purchased from Sigma (St. Louis, Missouri, USA) and was stored at 4°C. This reactant was carefully manipulated because it has a low vapor pressure and is potentially toxic by inhalation. Therefore, all the necessary precautions for safe handling were taken during the reactions under anhydrous conditions. PCL-diol (M_n = 1250 g mol^{-1} and M_n = 2000 g mol^{-1}) and PCL-triol (M_n = 900 g mol^{-1}) were purchased from Sigma-Aldrich (St. Louis, Missouri, USA) and were stored at room temperature.

Synthesis of Polyurethane and Film Casting

PCL-based PUs were produced by following a two-step process. In the first step, a series of NCO terminated prepolymers were prepared using HDI and PCL-diol or PCL-triol with NCO/OH ratio of 5 : 1, and reaction was carried out at 90°C under nitrogen atmosphere for 6 h. In the second step, viscous prepolymer was poured into glass molds and cured in vacuum oven at 95°C. Excess diisocyanate was used on purpose to obtain three-dimensional network structures via allophanate linkage formation as shown in Figure 1(A).

In the case of polyurethane ureas (PUU) synthesis, the same procedure was followed, but the second step was carried out in an oven at 95°C under atmospheric conditions so that the present humidity caused formation of additional biuret linkages as shown in Figure 1(B). Curing reactions were continued until free isocyanate peaks completely disappeared in the IR spectra which were obtained from the samples taken from the curing molds at different times and smeared on KBr pellets. The curing process took about 7 days, and the prepared PU films were kept in a vacuum desiccator until use. The thicknesses of the films were measured with a micrometer and were found to be in the range of 200–400 μm.

The coding of the obtained polymers identifies the composition. The first number gives the molar ratio of diisocyanate to polyol and the second number shows the molecular weight of the polyol. For example, PU5-1250 means the sample has the molar ratio of diisocyanate to polyol is 5, and PCL-diol has the molecular weight of 1250. The samples prepared under atmospheric pressure containing urea linkages were defined as PUU. When PCL-triol with molecular weight of 900 was used, 900T was added into the coding. In this study, four types of PUs were synthesized and coded as: PU5-1250, PU5-2000, PUU5-2000, and PU5-900T.

Characterization Methods

Chemical structure and presence of H-bonding in PU samples were evaluated by Perkin Elmer Spectrum 65 BX-FTIR-ATR Spectrometer (Massachusetts, USA). IR spectra of the film samples were obtained by using ATR attachment which has a ZnSe crystal. All spectra were collected using 32 scans with a resolution of 4 cm^{-1}. The spectral data were acquired by using ORIGIN 8 software.

Phase separation and height images (1 × 1 μm^2) of the samples were obtained by a Nanoscope Vecoo MultiMode V atomic force microscope (AFM, Santa Barbara, USA). Tapping mode AFM were performed under ambient conditions using a Silicon tip. AFM analyses were evaluated by using Gwyddion program, which was a free scanning probe microscopy data analysis software.[38]

Glass-transition temperature (T_g) and melting temperature (T_m) of the films were obtained by differential scanning calorimetry (DSC). Samples were sealed in standard aluminum capsules and thermal analyses were carried out using Scinco DSC N-650 (Seoul, Korea) at a heating rate of 10°C min^{-1} over the range of −100°C to 200°C under nitrogen atmosphere.

The thermal analyses were carried out using a Perkin Elmer Pyris 1 Thermogravimetric Analyzer (TGA) instrument (California, USA) under a heating rate 10°C min^{-1} under N_2 atmosphere.

Dynamic mechanical analyses (DMA) were carried out with Perkin Elmer Pyris Diamond DMA instrument (Shelton, USA). The samples were measured in an oscillatory tensile mode at a frequency of 1 Hz at a heating rate of 5°C min^{-1} under nitrogen atmosphere over the range of −100°C to 150°C. The

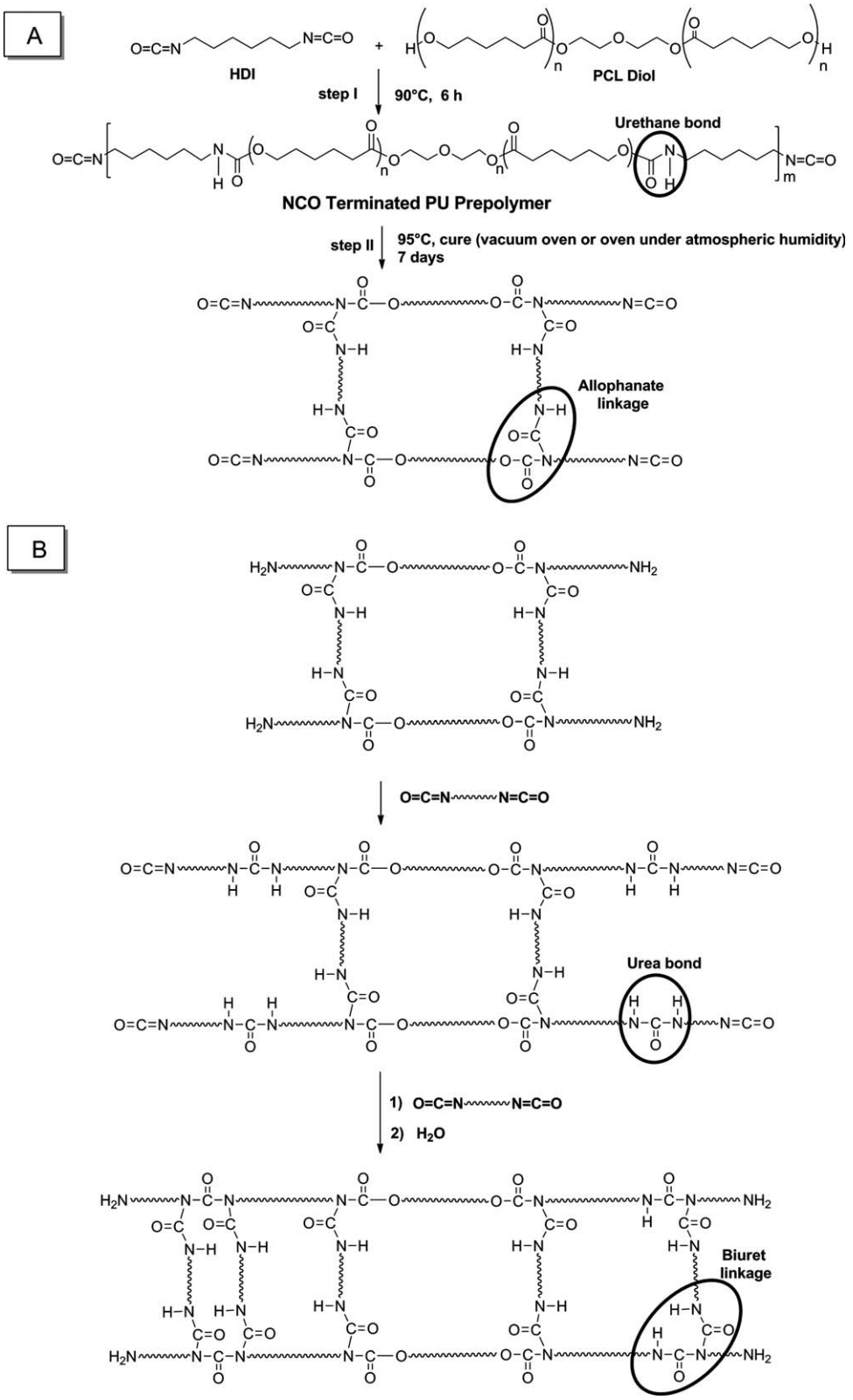

Figure 1. Chemical route for the synthesis of polyurethane (A) allophanate linkage formation, (B) urea and biuret linkage formation.

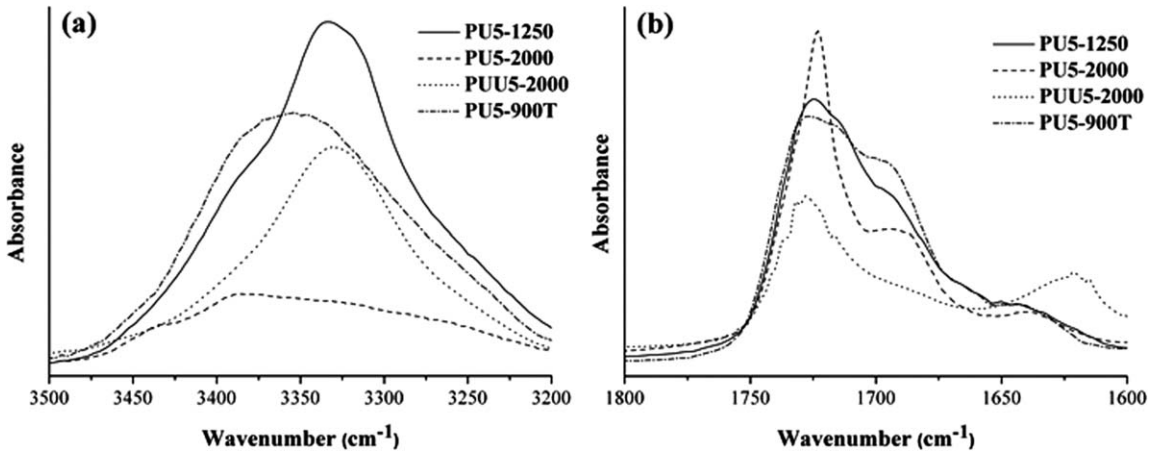

Figure 2. IR spectra for different segmented PU films: (a) N—H region; and (b) C=O region.

storage modulus (E') and loss modulus (E'') values were recorded against temperature.

X-Ray diffraction (XRD) measurements were measured with a Rigaku Ultima-IV X-Ray Diffractometer (Tokyo, Japan) with a copper target (λ = 1.54 Å), 40 kV 30 mA, equipped with a graphite monochromator. The data collection was performed in the range 2θ = 5–80° with a step of 0.02° at the rate of 2° min^{-1}.

Mechanical properties of the films were determined by a mechanical testing machine, Lloyd® LRX 5K (LLoyd Instruments, Fareham, Hampshire, UK), equipped with a 100 N load cell and a crosshead speed of 10 mm min^{-1}. For tensile tests, films were cut as dog bone shape (10 mm × 50 mm) and placed into instrument with gauge length of 10 mm ± 2 mm. The thickness of each sample was determined by a micrometer making measurements at different parts and the average values were estimated. At least 5 specimens for each type of films were tested. Ultimate tensile strength (UTS), Young's modulus (E), and percent elongation at break (EAB%) were calculated from stress–strain curves.

Static water contact angles of the films were measured by using a goniometer, CAM 200 (Helsinki, Finland). A total of 5 μL deionized water droplets were placed on the polymer surface using a microsyringe. At least 10 measurements were done and average values were obtained for each sample.

RESULTS AND DISCUSSION

FTIR-ATR Analysis

FTIR was used to study the effect of composition on the phase separation of the polymer samples. H-bonding in hard–hard segments (HS-HS) and hard–soft segments (HS-SS) can be seen as shifts to lower frequencies in both N—H and C=O stretching bands, which occur at 3500–3200 cm^{-1} and at 1800–1600 cm^{-1}, respectively (Figure 2). Deconvolution method was applied to determine the exact peak positions and areas of complex band envelopes arising from the relative contributions of the different groups. Both regions were deconvoluted by Peakfit Version 4.12 software and by considering peaks as a Gaussian–Lorentzian sum function to resolve more specific absorption peaks for individual characteristics of bands. Before fitting process, a flat baseline correction was performed in these ranges by subtracting the baseline. The correlation coefficients were more than 0.998. In polyester-based systems, there is a competition for hydrogen bonding between urethane–urethane or urea–urea and urethane–ester groups. If the interactions between HS and SS are dominant, then phase mixing of the systems occurs causing a reduction in the mechanical properties of the product.

The N—H Stretching Region

The deconvoluted spectra of N—H stretching region of the synthesized PUs are shown in Figure 3 and vibration bands at different frequencies are summarized in Table I. The peak positions obtained from deconvolution analysis are given in Table II. It is observed that N—H stretching region includes four main peaks. The first 3 peaks show free N—H bonds, H-bonded N—H bonds in HS-HS, and H-bonded N—H bonds in HS-SS. It was reported that H-bonds resulting from urethane groups in HS give rise to monodentate hydrogen bonding (which has a reported bond energy of 18.4 kJ/mol) and the ones resulting from urea linkages gives bidentate hydrogen bonding (which has a higher bond energy of 21.8 kJ/mol).[39] Peak IV represents an overtone of deformation vibration of N—H group increased by Fermi resonance in the system.

There are many definitions for Peak IV such as a two-phonon band,[40] an overtone of deformation vibration of N—H group increased by Fermi resonance,[41] and the N—H groups bonded with the carbonyl of urethane by forming a dual-cis bond.[42] Peak IV generally is not used to get any information about microphase separation. In the samples prepared in this study, the highest frequency of Fermi resonance was observed for PU5-900T. This resonance provides a mixing of a vibrational level in the chemically bonded molecule with near-resonant levels associated with vibrations against a van der Waals bond in the complex.[43] As a consequence of that, the highest branching of PU5-900T sample might cause a mixing of vibrational levels of the bonds and lead a shift to higher frequencies in peak IV.

The absorbance of the free N—H band (peak I) was observed at 3384 cm^{-1} for PU5-1250. As the length of SS chain increased (as in PU5-2000 and PUU5-2000) or branching was present (as

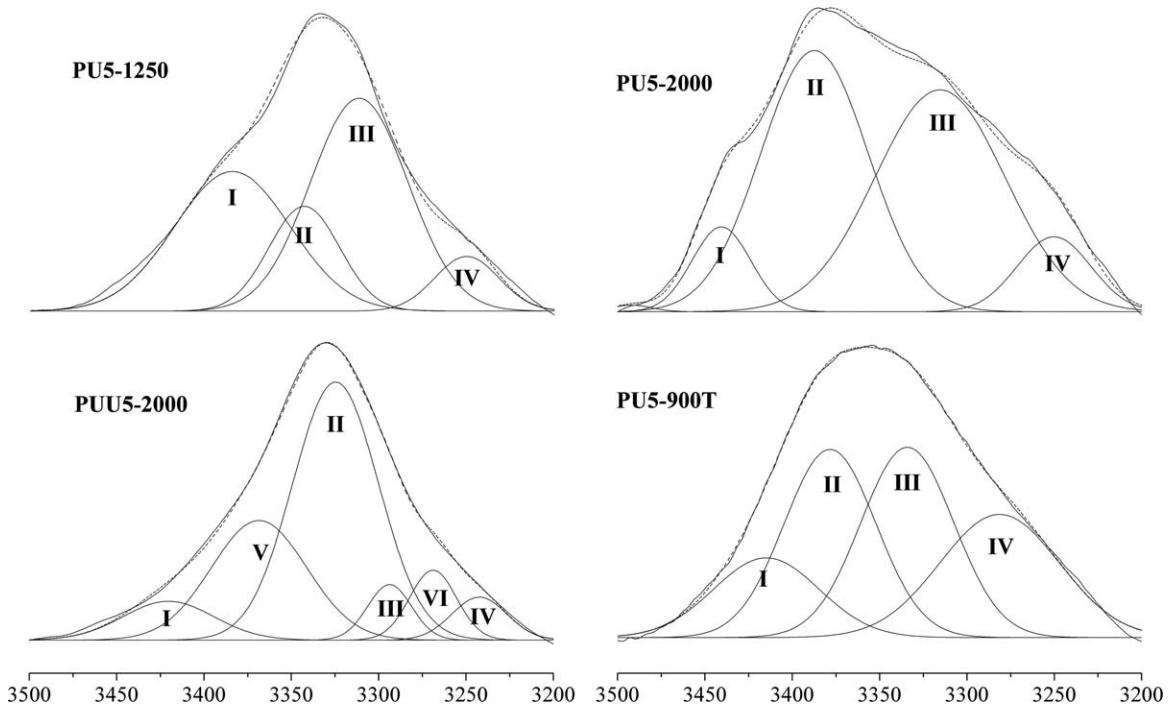

Figure 3. The deconvoluted N—H region of IR spectra. The original spectrum (solid line) is presented along with deconvolved spectrum (dashed line).

in PU5-900T), free N—H band shifted to higher frequencies, which shows variations in their environment because of different inter- or intra-molecular attractions.

Hydrogen bond formation between HS-HS is a driving force in phase segregation. It was reported that shifting of absorbance peaks to lower frequencies demonstrates increase in the bond strength and decrease in average H-bond length.[44] When PU5-1250 and PU5-2000 are compared, longer polyol chains caused an increase in frequencies of N—H bonds of urethane groups in the peaks II and III. This could be concluded as a decrease in the bond strength upon increase in the chain length. As the chain length gets longer, the number of possible conformational rotations increases and this affects the bond strength.

Table I. Infrared Stretching Band Assignments of N—H Group in PU Samples

Peak	Wavenumbers (cm^{-1})	Assignation
I	3440–3384	free N—H (urethane)
II	3388–3324	H bonded N—H in HS-HS (urethane)
III	3334–3294	H bonded N—H in HS-SS (urethane or urea)
IV	3281–3242	overtone of C=O and N—H (Fermi resonance)
V	3368	free N—H (urea)
VI	3269	H bonded N—H in HS-HS (urea)

For PUU5-2000 sample, the presence of urea groups created two additional peaks that represent free and H-bonded N—H in urea groups. For this sample, the lowest frequency (3324 cm^{-1}) was observed for peak II which indicates the strongest HS-HS interactions in urethane groups. Hydrogen interactions in both urethane and urea groups enhanced formation of stronger H-bonds. The weakest H-bond between hard–soft segments was observed for PU5-900T (peak III at 3334 cm^{-1}). It was concluded that polymer branching prevented the chains to come close to each other and, therefore, weakened the strength of the H bonds. In addition to knowledge of frequency shifts, band areas also give extra information about the amount of phase separation. N—H band area for each vibration was estimated on the basis of total N—H stretching band area, and summarized in Table III.

The highest percentages of free N—H groups in urethane linkages were observed for PU5-1250 sample having 33.6% (peak I) of the total area. The increase in the chain length of polyol (PU5-2000) decreased the peak area of free N—H to 8.7%, because free N—H groups prefer H-bonding with C=O groups in urethane linkages (43.1%).

For PUs, phase segregation can be estimated from the peak area ratios of HS-HS to HS-SS interactions. When all samples are compared, the lowest HS-HS interactions (15.7%) and the highest HS-SS interactions (43.2%) were obtained for the PU5-1250 sample. The results show that PU5-1250 has the minimum phase separation.

Urea groups in PUU5-2000 lead the highest HS-HS interactions (49.1% from urethane and 7.3% from urea) among all samples. On the other hand, HS-SS interactions were much lower and,

Table II. Deconvolution Results of Peak Position of N—H Region for All Samples

	Peaks and peak position (cm^{-1})					
Sample	I (Free) Urethane	II (HS-HS) Urethane	III (HS-SS) Urethane or urea	IV Fermi resonance	V (Free) Urea	VI (HS-HS) Urea
PU5-1250	3384	3343	3311	3250	-	-
PU5-2000	3440	3388	3317	3251	-	-
PUU5-2000	3420	3324	3294	3242	3368	3269
PU5-900T	3414	3378	3334	3281	-	-

therefore, PUU5-2000 exhibited the maximum phase segregation and minimum phase mixing behavior.

If PU5-900T and PU5-1250 are compared, the branched and the shorter polyol improved HS-HS interactions (a decrease in the peak I area and an increase in peak II area). The branched structure of polyol in PU5-900T leads to approximately equal phase mixing (30.4%) and phase separation (29.8%). The highest peak IV area was observed for this branching sample as a result of Fermi resonance arising from the mixing of vibrational levels of the bonds.

As conclusion, the presence of longer SSs for crosslinked PU production allows forming readily hydrogen bonds in HS-HS resulting in better phase separation. In addition, the presence of urea groups in the polymer structure further increased phase separation in polymer structure. From the obtained data, it was concluded that the phase separation order was given as: PUU5-2000 > PU5-2000 > PU5-900T > PU5-1250.

The C═O Stretching Region

The C═O stretching vibrations are helpful to evaluate complementary results to the N—H stretching region. The existence of hydrogen bonding prolongs the carbonyl bond and this results in shifting to lower frequencies in stretching vibration compared with that of the free C═O band.[45] The deconvoluted spectra of C═O region is given in Figure 4. Although, the chemical structures of the urethane groups are identical in different compounds, there is a remarkable difference in their IR spectra. PU samples involve five characteristic absorption peaks in this region, whereas PUU samples have two additional peaks. Table IV provides information about different peaks present in this region and Table V gives deconvolution results of the peak positions of C═O region. The absorbance of the free carbonyls in ester and urethane groups (peaks I and III) shifted to higher frequencies as the chain length and branching of polyol increased. This is resulted by the variations in the environment of free C═O groups.

Lower frequencies observed for HS-SS interaction of ester carbonyl and HS-HS interactions of urethane carbonyls demonstrated stronger hydrogen bonding. Therefore, PU5-1250 and PU5-900T have enhanced HS-SS and HS-HS interactions because they have the lower frequencies compared with PU5-2000 and PUU5-2000. This can be concluded as the presence of shorter polyol chain and branching lead to stronger H bonding. For PUU5-2000, the highest frequencies were observed for peaks II and IV. This indicates weak hydrogen bonding of ester and urethane groups, but on the other hand, the presence of HS-HS interactions coming from urea carbonyls makes the system stronger (as will be shown in mechanical properties part).

Table VI represents a comparison of the relative amounts of C═O groups in the polymer structure. The experimental results revealed that incorporation of a triol SS into PU structure accomplished maximum reduction in H-bond formation in HS-HS. PU5-900T creates a least favorable hydrogen bonding interaction in HS (4.6%) when compared with the all remaining materials. It is also observed that almost half of the carbonyl groups (45.0%) are free in PU5-1250. However, the presence of urea groups in PUU5-2000 significantly decreased the amount of free ester carbonyl groups down to 8.7%. For PUU sample, urethane and urea carbonyls attributed into HS-HS interactions (total ~35%). Therefore, PUU5-2000 possessed the highest microphase separation.

On the basis of all IR analysis, it may be concluded that the nature of polyol (functionality and molecular weight) used for PU synthesis have great influence on phase segregation, which consequently results a new morphology with altered hydrogen bonding. Branched polyol in PU5-900T end up with a reduction

Table III. Deconvolution Results of Peak Area of N—H Region for All Samples

	Peaks and peak areas (%)					
Sample	I (Free) Urethane	II (HS-HS) Urethane	III (HS-SS) Urethane or urea	IV Fermi resonance	V (Free) Urea	VI (HS-HS) Urea
PU5-1250	33.6	15.7	43.2	7.5	-	-
PU5-2000	8.7	43.1	38.5	9.7	-	-
PUU5-2000	7.8	49.1	5.4	5.2	25.2	7.3
PU5-900T	14.5	29.8	30.4	25.3	-	-

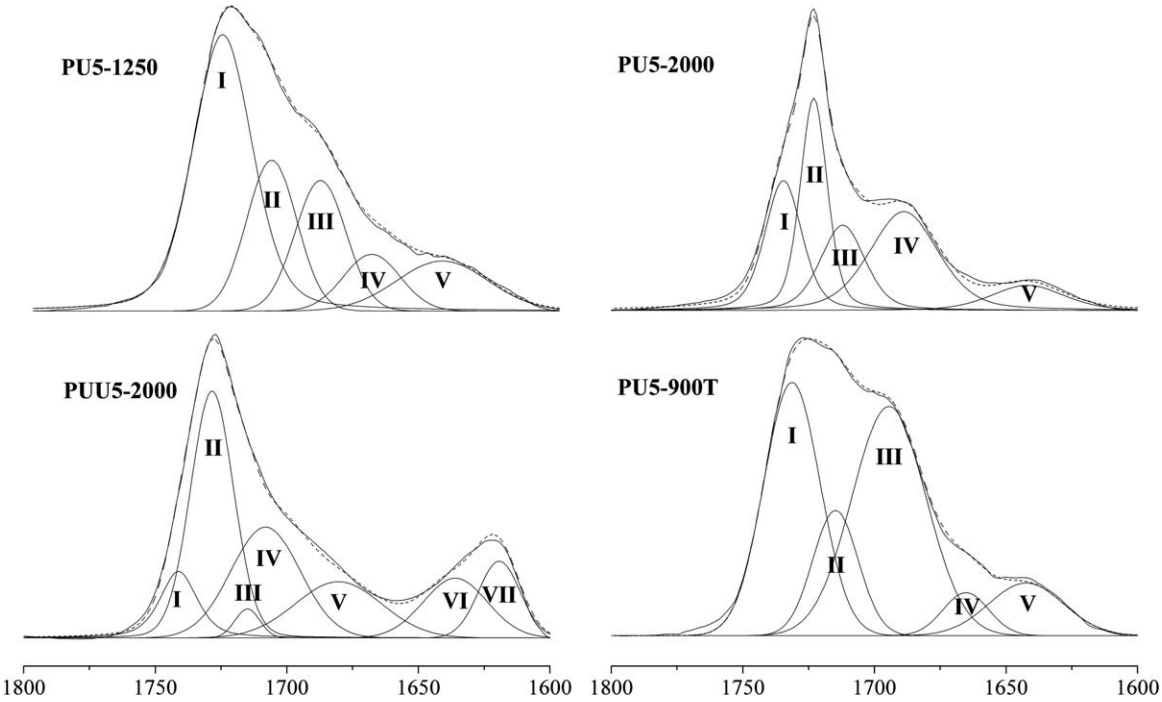

Figure 4. The deconvoluted C═O region of IR spectra. The original spectrum (solid line) is presented along with deconvolved spectrum (dashed line).

in phase segregation. The existence of longer SS in polymers increased concentration of H-bonds in HS-HS. In PUU5-2000, it is obvious that urea groups make stronger H-bonds between HS-HS as expected. When comparing the area of H-bonds in HS-HS (peak IV) and H-bonds in HS-SS (peak II), microphase segregation can be given as in the following order: PUU5-2000 > PU5-2000 > PU5-1250 > PU5-900T.

For PU5-1250 and PU5-900T samples, the order of phase separation is different from the results of N—H region. As explained previously, peak IV of N—H region is not used to get information about microphase separation. But in this case, the lowest value of microphase segregation observed for PU5-900T, which is most probably the high value of Fermi resonance.

AFM Analysis

AFM phase images of all polymer samples showed phase separation as brighter regions for HS, and darker regions for SS as described in literature.[46] For PU5-1250, aggregation of hard domains was observed as bright and isolated islands. This shows effective packing of HS domains [Figure 5(a,b)]. Increase in chain length of PCL (as in PU5-2000), did not affect the size and the distribution of the HS domains. For both samples, distinct interfaces between different phases were observed [Figure 5(b,d)]. In PUU samples (PUU5-2000), the existence of the brightest regions demonstrates the presence of the most effectively packed hard domains, whereas dark region showed inhomogeneous matrix formation [Figure 5(e,f)]. In the branched polyol based PU samples (PU5-900T), hard domains were very small in size and homogeneously distributed in the soft phase. HS domains had clear connectivity and were not isolated from each other [Figure 5(g,h)].

Table IV. Infrared Stretching Band Assignments of C═O Group in PU Samples

Peak	Wavenumber (cm^{-1})	Assignation
I	1741-1728	free C═O (ester)
II	1729-1709	H-bonded C═O in HS-SS (ester)
III	1713-1691	free C═O (urethane)
IV	1708-1665	H-bonded C═O in HS-HS (urethane)
V	1680-1642	C═O in allophanate and/or biuret
VI	1636	Free C═O (urea)
VII	1620	H-bonded C═O in HS-HS (urea)

DSC Analysis

DSC thermograms obtained for pure polyols with corresponding polymers were illustrated in Figure 6. DSC thermal behavior was apparent in two temperature ranges, which were T_g and T_m of SS. Polymer films were all rubbery form because of their relatively low T_g. As seen in Table VII, a significant increase in T_g of all polymers was observed by polymer formation.

T_g values of PU5-1250 (−52.7°C), PU5-2000 (−56.9°C), and PUU5-2000 (−58.3°C) were significantly lower than that of PU5-900T (−24.8°C). This is due to better phase separation in these samples compared with branched polymer, as evidenced by IR analysis. In general, increase in the T_m values can be described in terms of the improved interactions and regular orientations of molecular chains as the molecular weights of polyols increases. The highest T_g (at −24.8°C) and the smallest T_m (at −1.1°C) may have been caused by shorter chain length and more number of crosslink sites present in PU5-900T. It can be

Table V. Deconvolution Results of Peak Position of C=O Region for All Samples

	Peaks and peak position (cm^{-1})						
Sample	I (Free) Ester	II (HS-SS) Ester	III (Free) Urethane	IV (HS-HS) Urethane	V Allophanate (and/or biuret)	VI (Free) Urea	VII (HS-HS) Urea
PU5-1250	1728	1709	1691	1671	1643	-	-
PU5-2000	1735	1723	1712	1689	1642	-	-
PUU5-2000	1741	1729	1713	1708	1680	1636	1620
PU5-900T	1731	1715	1694	1665	1642	-	-

concluded that as phase mixing increases, T_g of the material shifted to higher temperatures because of H-bond fixation of polyol chains. Reduction in T_m can also be explained by phase mixing, which disrupts well-ordered orientation in polyol components.

When the melting enthalpies of the materials are compared, a significant decrease by forming polymers were observed compared with the unreacted PCL molecules. For both PCL diol 1250 and PCL diol 2000, the enthalpy values are higher than 100 J/g, and dropped about 4 or 5 times. Formation of urethane bonds decreased the bond strength between the macro chains and prevented their proper organization in PCL structure. As a conclusion, the molecular weight of the polyol is the dominant factor for the T_m of SSs. However, phase separation in the polymer structure is another factor affecting thermal behavior of samples.

TGA Analysis

Thermal degradation behaviors of segmented PUs over the temperature range of 30–600°C were displayed in Figure 7 and decomposition temperatures for different phases were summarized in Table VIII. For all polymers, thermal decomposition occurred in two steps. The initial decomposition peaks (T_1) around 373–381°C correspond to thermal degradation of HSs. The peaks around 442–458°C (T_2) were attributed to decomposition of SSs. PU5-900T sample had the lowest thermal stability compared with the other samples having the lowest decomposition temperatures for both HSs (at 373°C) and SSs (at 442°C). For this sample, phase segregation was significantly less than the other samples and most probably this also caused a decrease in thermal stability.

DMA Analysis

Dynamic mechanical analysis is an effective technique in the characterization studies of viscoelastic materials where an oscillating force is applied to the material. Figure 8 compares the viscoelastic properties of the crosslinked films as a function of temperature at 1 Hz in terms of E' and E''. In this study, temperature was ramped from −100°C to a temperature at which the sample became too soft. Multiple segmental relaxations in DMA confirm the presence of hetero-phase morphology in the samples. Table IX listed transitions obtained from storage modulus.

PU5-1250 and PU5-900T displayed two phase morphologies, with well-defined SS glass transitions followed by a fairly long and temperature insensitive rubbery plateau. PU5-1250 and PU5-900T, both display a fairly broad SS T_g values starting from −60°C and from −30°C, respectively, and extending up to 0°C. These were obtained from the inflection points of storage modulus-temperature curves. In both cases, this change is a result of significant amount of phase mixing. Following this SS, T_g transition is a rubbery plateau (starting from 0°C and extending up to about 150°C), whose breadth, average plateau modulus value, and temperature sensitivity depend upon the level of phase segregation and the type of hydrogen bonding within the hard phase.

When we consider all PU samples, different thermo-mechanical behaviors were observed. DMA of PU5-2000 showed three phase morphology. The lower α relaxation in E' (−52°C) corresponds to the T_g of PCL-diol 2000 segment, the presence of a second relaxation due to HS T_g at about 39°C, and another phase at 1°C showing T_g for mixed phase. Furthermore, the

Table VI. Deconvolution Results of Peak Area of C=O Region

	Peaks and peak area (%)						
Sample	I (Free) Ester	II (HS-SS) Ester	III (Free) Urethane	IV (HS-HS) Urethane	V Allophanate (and/or biuret)	VI (Free) Urea	VII (HS-HS) Urea
PU5-1250	45.0	18.9	16.6	8.1	11.4	-	-
PU5-2000	21.1	25.3	16.7	29.2	7.7	-	-
PUU5-2000	8.7	29.6	2.1	23.6	14.1	10.8	11.1
PU5-900T	33.3	13.3	39.6	4.6	9.2	-	-

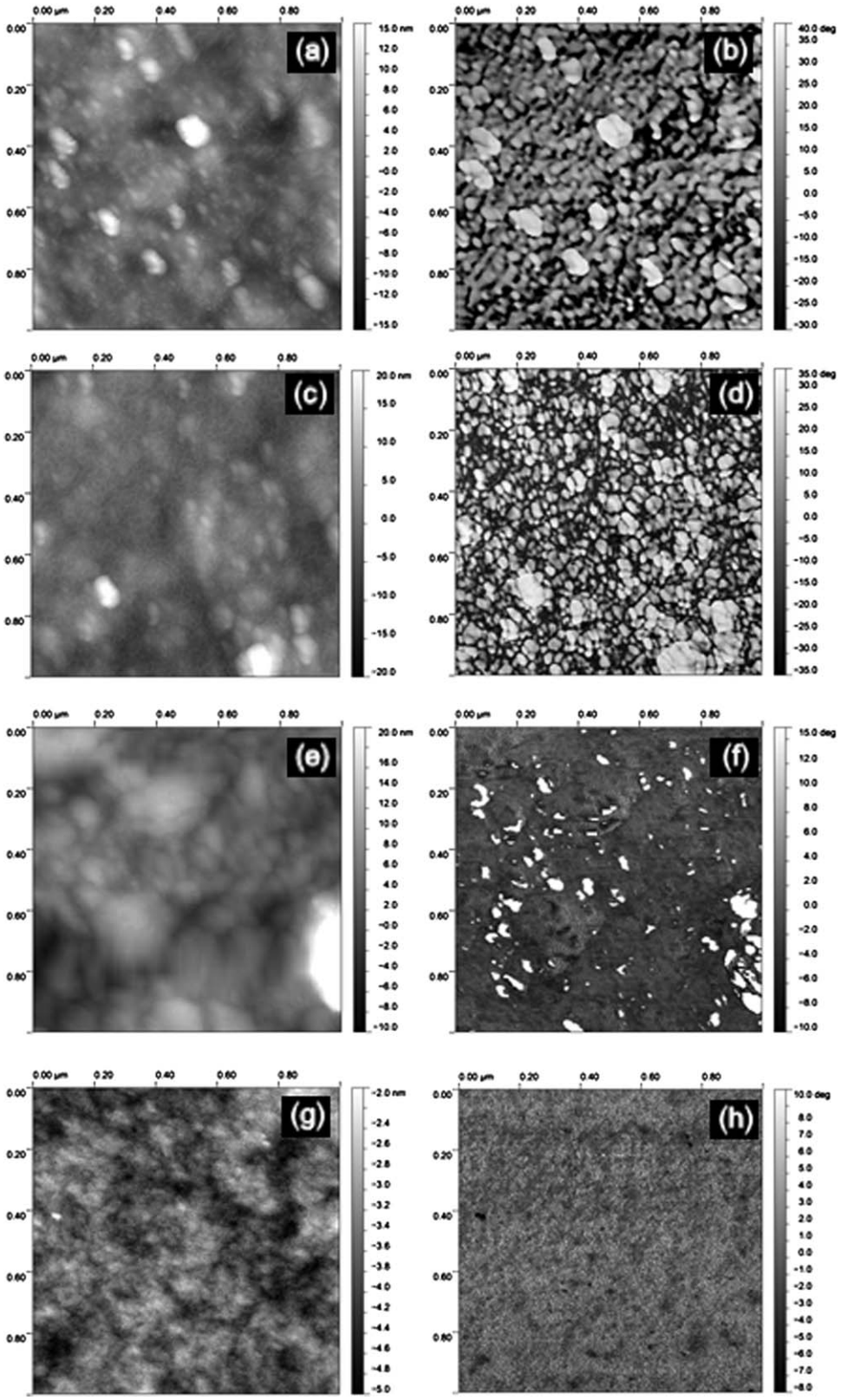

Figure 5. AFM height images (left) and phase images (right) of 1 μm^2 of PU film surfaces: (a,b) PU5-1250; (c,d) PU5-2000; (e,f) PUU5-2000; and (g,h) PU5-900T.

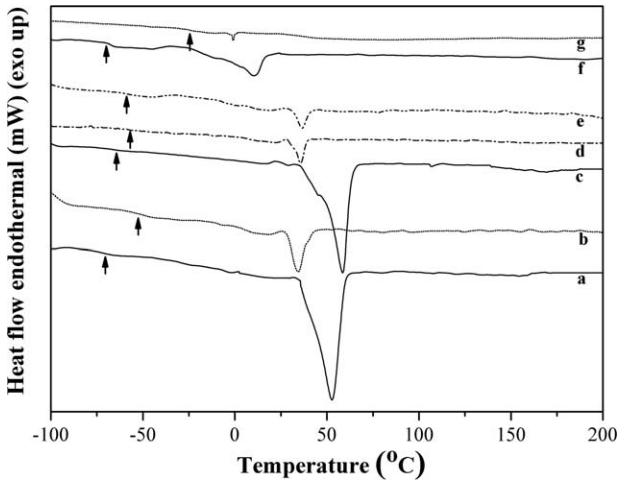

Figure 6. DSC thermograms: (a) PCL-diol 1250; (b) PU5-1250; (c) PCL-diol 2000; (d) PU5-2000; (e) PUU5-2000; (f) PCL-triol 900; and (g) PU5-900T.

DMA response of PUU5-2000 shows α relaxation in E' at −59°C and the second relaxation at 1°C assigned to HS relaxations and mixed phase relaxation at −10°C. On the other hand, two other small deviations were observed in the rubbery plateau (which has an increasing slope) at 46°C and 59°C. The increase in the slope demonstrates strengthening of the material with temperature. This might be a result of continuing curing or new orientations of the macrochains forming new interactions. It is possible that two different crystalline structures formed between HS domains, such as urea–urea and/or urethane–urethane interactions. PUU5-2000 displays the highest modulus of 1×10^8 Pa, where it may be due to the higher crosslinking density and crystallinity, higher aspect ratio of the HS crystallites in the phase segregated material.

The highest T_g (−26°C) was observed for PU5-900T which has branched polyol in the structure. A plausible explanation is that the branching discourages HS packing and thereby promotes mixing with the SSs. The IR data presented earlier clearly supported the hypothesis for disordered HS phase.

PUs are commonly used in the production of medical devices ranging from catheters to total artificial hearts. This uses the importance of dynamical mechanical behavior at room temperature and body temperature. Therefore, the storage and loss modulus values of the prepared PU films were determined at both 25°C and 37°C, and are listed in Table X.

Table VII. Results of the DSC Analysis of PU (±SD, $n = 3$)

Sample	T_g (°C)	T_m (°C)
PCL diol 1250	−69.4 ± 1.6	52.9 ± 1.4
PU5-1250	−52.7 ± 2.5	21.4 ± 2.6
PCL diol 2000	−64.1 ± 1.8	58.5 ± 2.5
PU5-2000	−56.9 ± 1.9	29.6 ± 1.5
PUU5-2000	−58.3 ± 2.1	36.7 ± 2.1
PCL triol 900	−68.7 ± 1.2	15.2 ± 2.3
PU5-900T	−24.8 ± 3.1	−1.1 ± 1.8

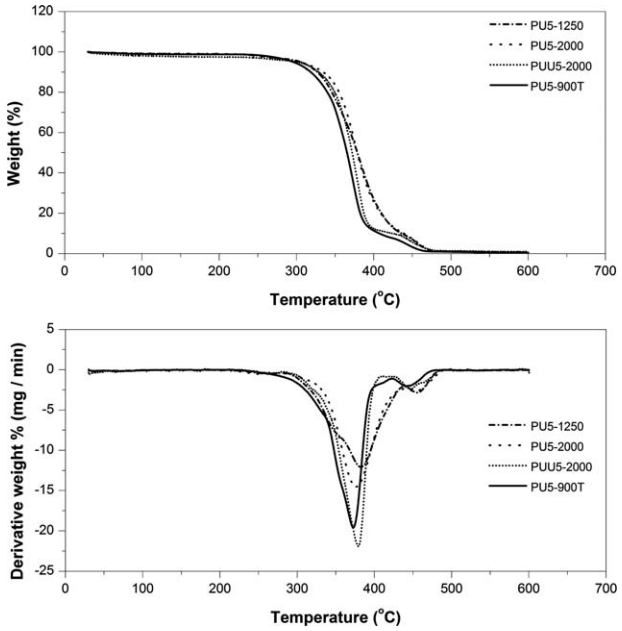

Figure 7. TGA results for all polyurethanes, obtained at a heating rate of 10°C/min.

PU5-2000 exhibits the highest value for E' at both temperatures in the rubbery plateau region of the curve. Moreover, at 37°C, PU5-2000 has the highest storage value (20.4 MPa) at body temperature and the storage modulus was 12–14 times higher than the loss modulus (0.8 MPa). This meant that the energy change required for displacement was mainly reversible. According to DMA analysis, resulted from the phase separation morphology, existence of a multitude of transitions, and their relative glass transition values, the order of phase segregation was given as: PUU5-2000 > PU5-2000 > PU5-1250 > PU5-900T.

XRD Analysis

X-Ray diffraction analysis was carried out to examine long-range orders produced as a consequence of very short-range interactions. The relative crystallinity among polymer samples was compared in Figure 9 at a range of 5–45°.

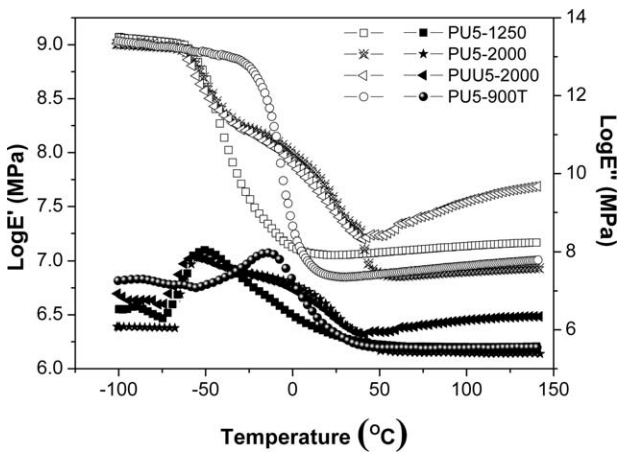

Figure 8. DMA curves of PUs (conditions: 5C/min, 1 Hz, film in tensile mode).

Table VIII. TGA Results of Polyurethanes

Sample	T_1 (°C)	T_2 (°C)
PU5-1250	381	457
PU5-2000	376	458
PUU5-2000	378	447
PU5-900T	373	442

Because solvent was not used in the polymer synthesis, proper films of polyols were not obtained for the XRD analysis. Therefore, it was used for the characteristic peaks of PCL from the literature. According to literature, the characteristic peaks of PCL (semi-crystalline) are at $2\theta = 21°$ and $2\theta = 23.5°$.[47] For PU samples, a broad diffraction peak can be obviously observed with the maxima's in the range of $2\theta = 20.28°–20.88°$ indicating PCL crystalline phase, not identical with those of pure PCL. It can be concluded that the orderly arrangement of crystalline phase was preserved in the PU samples after crosslinking. On the other hand, the crystallinity of the branched polymers was lower than for their linear analogues due to shorter chain length and the increase in the number of crosslink sites disrupting the SS crystallinity.

In literature, the peak located at around $11°2\theta$ is assigned to the crystallinity of HSs. In this study, no sharp peak due to crosslinking is found in any diffractogram, but the peak correspond to the HS crystallinity appears as a shoulder at around $11°2\theta$ because of band overlapping. In all PU, the positions of the PCL crystals remain almost constant though the intensity of the peaks indicating crystallinity content increased according to following order: PUU5-2000 > PU5-2000 > PU5-1250 > PU5-900T.

Mechanical Properties

The mechanical properties such as ultimate tensile strength (UTS), elastic modulus (E), and elongation at break (ε) values were measured and related to chemical composition. Tensile test results are illustrated in Figure 10 and summarized in Table XI.

PU films were flexible with tensile strengths ranging from 2.7 MPa to 16.3 MPa, modulus 7.9 MPa to 56.5 MPa, and breaking strains from 63.7% to 653.8%. As the molecular weight of polyol was gradually changed from 1250 to 2000, the elongation showed a significant increase from 85.9% to 432.3%. With the addition of urea linkages to the polymer structure, polymer elongation increased about 50% (653.8%). This is due to much stronger hydrogen bonding between urea groups when compared with urethanes. UTSs of the polymers showed strong dependence on the strength of the hydrogen bonding between HSs and average molecular weight of the PCL SS. As expected lower phase segregated polymers, PU5-1250 and PU5-900T displayed the lowest UTS of 2.7 MPa; on the other hand, more phase separated polymer, and PU5-2000 had almost twice as high tensile strength values around 5.6 MPa.

Table IX. Transitions Obtained from Storage Modulus at 1 Hz

	Transitions[a]		
Sample	T_{g1} (°C)	T_{gM} (°C)	T_{g2} (°C)
PU5-1250	−50	-	-
PU5-2000	−52	1	39
PUU5-2000	−59	−10	1
PU5-900T	−26	-	-

[a] T_{g1}: Soft segment glass transition temperature; T_{g2}: hard segment glass transition temperature; T_{gM}: mixed phase glass transition temperature.

Table X. Storage and Loss Modulus of PU at 1 Hz at 25°C and 37°C

Sample	E' at 25°C (MPa)	E' at 37°C (MPa)	E'' at 25°C (MPa)	E'' at 37°C (MPa)
PU5-1250	11.3	11.5	0.7	0.5
PU5-2000	33.8	20.4	2.4	0.8
PUU5-2000	27.4	16.5	1.8	0.8
PU5-900T	7.2	7.2	0.8	0.4

As discussed previously, the characteristic of the crosslinked polymers were governed by the nature of the constituent monomers and their relative concentration, but also by the resultant distance between the crosslinking points. If the interactions between crosslink points are tight, the chain length between the crosslinks is short and the higher modulus is observed for this type of polymers. Thus, crosslinking contributed to enhancing elastomeric properties of the polymers by recover after deformation. PUU5-2000 exhibits remarkable elongation (653.8%) at break. However, PU5-1250 exhibits lower (85.9%) and PU5-900T has even more lower elongation (63.7%). The primary consequences of increasing the molecular weight of the soft block for a given overall molar ratio of hard block to polyol block, as in the case of PU5-1250 and PU5-2000, results in a decrease in modulus from 9.9 MPa to 7.9 MPa and an increase in elongation from 85.9% to 432.3%.

Among PUs, urea-based PU suggests better mechanical properties over remaining materials, which reflect the regularity of its chain structure and its ability to crystallize upon extension with the addition of urea bonds in PUU5-2000. A polyol having a more symmetrical structure will enhance the formation of organized structures in HS domains, and thus, more complete phase segregation. Because PU5-900T possesses highly branched structure and large number of reactive end groups composed of three armed SS prevents formation of ordered structures, resulting in decrease in tensile strength (2.7 MPa) and elongation (63.7 MPa). Therefore, by appropriate variations in chemical

Table XI. Tensile Properties of PU Films (±SD, $n = 5$)

	Mechanical properties		
Sample	UTS (MPa)	E (MPa)	ε (%)
PU5-1250	2.7 ± 0.4	9.9 ± 1.5	85.9 ± 21.4
PU5-2000	5.6 ± 1.7	7.9 ± 1.8	432.3 ± 145.8
PUU5-2000	16.3 ± 4.3	56.5 ± 6.8	653.8 ± 116.7
PU5-900T	2.7 ± 0.2	8.1 ± 1.2	63.7 ± 12.9

Table XII. Water Contact Angle Values (±SD, $n = 5$)

Sample	Water contact angle (°)
PU5-1250	79.3 ± 3.5
PU5-2000	72.7 ± 1.6
PUU5-2000	82.4 ± 2.4
PU5-900T	78.1 ± 1.2

structure, molecular weight, and composition, it is possible to obtain polymers with different strength, Young's modulus, and elasticity for a wide range of mechanical properties. In general, increase in molecular weight of SS contributed to better mechanical properties. The tensile force acting on the material might have led to better orientation and/or crystallization within the HS domains. The elastomeric properties of the PU depend on polyol type and as a consequence of the alteration in hydrogen bonding characteristics.

Water Contact Angles

The effect of composition on surface hydrophilicity was evaluated in a semi-quantitative manner through the use of contact angle measurements. It is known that to regulate the surface free energy is possible by the selection of appropriate substrates.[48] According to Table XII, the static water contact angles of the prepared films varied from 72.7° to 82.4°.

A decrease in contact angle was observed in PU5-2000. The largest contact angle obtained for the PUU5-2000 indicating the presence of a largest hydrophobic surface. It was expected that the longer PCL incorporated in the SS of the PUs define a more hydrophobic behavior, because of the existence of more hydrocarbons sequence. However, the insertion of excess isocyanate compounds altered the surface wetting characteristic of the polymeric matrix with reducing the extent of polar groups on the surface by introducing allophanate and/or biuret linkages.

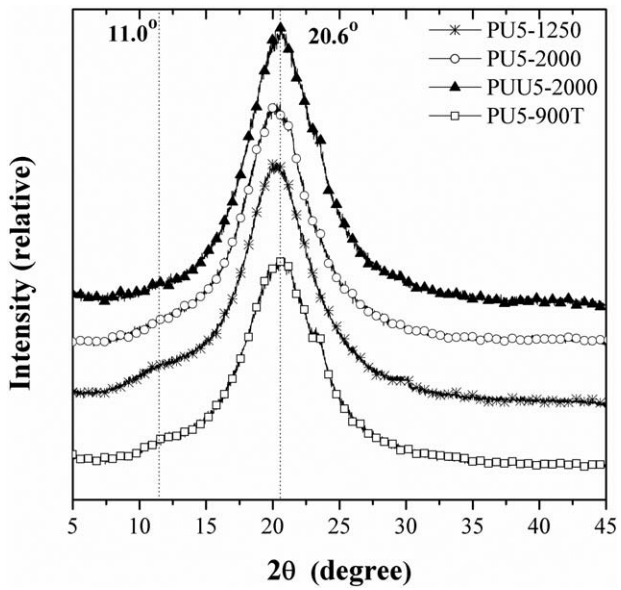

Figure 9. The XRD curves of different PU films at range of 5–45°.

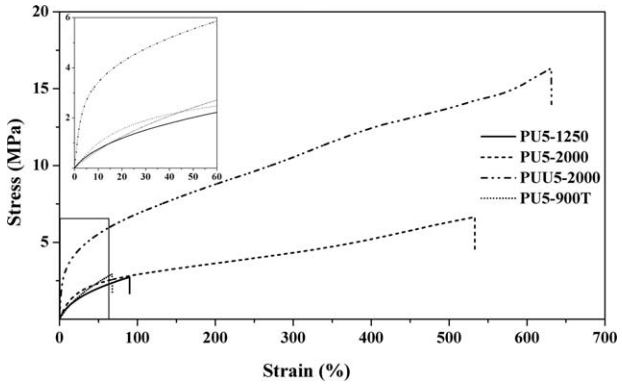

Figure 10. Stress–strain graphs of PU.

CONCLUSIONS

In this study, crosslinked PU and PUU films were synthesized without using any catalyst, solvent, or chain extender. Development of polymers for biomedical applications requires optimization of their properties. The results showed that polymers synthesized from different molecular weights as well as different SS structures exhibit different interactions in the molecular chains. These polymers can be easily fashioned to obtain required properties using environmentally friendly methods. Thermal decomposition temperatures of polymers did not show significant difference among each other because they were all crosslinked structures. AFM analyses showed that depending on the type and molar mass of polyol, hard and soft domains differ. This type of phase segregation effects thermal and mechanical behaviors of the resultant polymers. By considering the findings of this study, it can be concluded that crosslinked films with longer PCL chains in the SS have better tensile properties. It was also found that urea-based PUs has remarkable tensile properties. With increasing number of terminal groups and branching, crystallinity of polymers decreases. Microphase separation improved flexibility and strength of final product. Results showed that PUs with various properties can be synthesized via environmentally friendly process without using any solvent or catalyst.

ACKNOWLEDGMENTS

The authors are grateful to Engin Özkol (Department of Chemical Engineering, METU, Turkey) for his help in the use of Peakfit Version 4.12 software and thank to METU Central Laboratory for characterization analyses of AFM, DMA, and XRD. This study was supported by METU-BAP-07-02-2011-00-01.

REFERENCES

1. Furukawa, M.; Shiiba, T.; Murata, S. *Polymer* **1999**, *40*, 1791.
2. Bogdanov, B.; Toncheva, V.; Schacht, E. *J. Therm. Anal. Calorim.* **1999**, *56*, 1115.
3. Miller, C. E.; Edelman, P. G.; Ratner, B. D.; Eichinger, B. E. *Appl. Spectrosc.* **1990**, *44*, 581.
4. Ozdemir, Y.; Hasirci, N.; Şerbetçi, K. *J. Mater. Sci.: Mater. Med.* **2002**, *3*, 1147.

5. Lee, H. S.; Wang, Y. K.; Hsu, S. L. *Macromolecules* **1987**, *20*, 2089.
6. Sharifpoor, S.; Simmons, C. A.; Labow, R. S.; Paul Santerre, J. *Biomaterials* **2011**, *32*, 4816.
7. Alperin, C.; Zandstra, P. W.; Woodhouse, K. A. *Biomaterials* **2005**, *26*, 7377.
8. Sharifpoor, S.; Labow, R. S.; Santerre, J. P. *Biomacromolecules* **2009**, *10*, 2729.
9. Riboldi, S. A.; Sampaolesi, M.; Neuenschwander, P.; Cossu, G.; Mantero, S. *Biomaterials* **2005**, *26*, 4606.
10. Longo, U. G.; Lamberti, A.; Maffulli, N.; Denaro, V. *Br. Med. Bull.* **2010**, *94*, 165.
11. Laurencin, C. T.; Freeman, J. W. *Biomaterials* **2005**, *26*, 7530.
12. Greenwood, J. E.; Dearman, B. L. *J. Burn Care Res.* **2012**, *33*, 7.
13. Grad, S.; Kupcsik, L.; Gorna, K.; Gogolewski, S.; Alini, M. *Biomaterials* **2003**, *24*, 5163.
14. Chia, S. L.; Gorna, K.; Gogolewski, S.; Alini, M. *Tissue Eng.* **2006**, *12*, 1945.
15. Hafeman, A. E.; Li, B.; Yoshii, T.; Zienkiewicz, K.; Davidson, J. M.; Guelcher, S. A. *Pharm. Res.* **2008**, *25*, 2387.
16. Gogolewski, S.; Gorna, K.; Turner, A. S. *J. Biomed. Mater. Res. A* **2006**, *77*, 802.
17. Aksoy, A. E.; Hasirci, V.; Hasirci, N. *Macromol. Symp.* **2008**, *269*, 145.
18. Kamısoglu, K.; Aksoy, E. A.; Akata, B.; Hasirci, N.; Bac, N. *J. Appl. Polym. Sci.* **2008**, *110*, 2854.
19. Guelcher, S. A.; Gallagher, K. M.; Didier, J. E.; Klinedinst, D. B.; Doctor, J. S.; Goldstein, A. S.; Wilkes, G. L.; Beckman, E. J.; Hollinger, J. O. *Acta Biomater.* **2005**, *1*, 471.
20. Kayirhan, N.; Denizli, A.; Hasirci, N. *J. Appl. Polym. Sci.* **2001**, *81*, 1322.
21. Hasirci N. Polyurethanes. In High Performance Biomaterials; A Comprehensive Guide to Medical and Pharmaceutical Applications; Szycher, M., Ed.; Technomic Publishing Co: Lancaster, Pennsylvania, USA, **1991**; pp 71–91.
22. Guelcher, S. A. *Tissue Eng. Part B* **2008**, *14*, 3.
23. Sheth, J. P.; Klinedinst, D. B.; Wilkes, G. L.; Yilgor, I.; Yilgor, E. *Polymer* **2005**, *46*, 7317.
24. Burke, A.; Hasirci, N. *Adv. Exp. Med. Biol.* **2004**, *553*, 83.
25. Zhang, L.; Jiang, Y.; Xiong, Z.; Liu, X.; Na, H.; Zhang, R.; Zhu, J. *J. Mater. Chem.* **2013**, *1*, 3263.
26. Xue-Hai, Y.; Nagarajan, M. R.; Grasel, T. G.; Gibson, P. E.; Cooper, S. L. *J. Polym. Sci. Polym. Phys. Ed.* **1985**, *23*, 2319.
27. Wen, T. C.; Wu, M. S. *Macromolecules* **1999**, *32*, 2712.
28. Kojio, K.; Kugumiya, S.; Uchiba, Y.; Nishino, Y.; Furukawa, M. *Polym. J.* **2009**, *41*, 118.
29. Kutay, S.; Tincer, T.; Hasirci, N. *Br. Polym. J.* **1990**, *23*, 267.
30. Hasirci, N.; Aksoy, E. A. *High Perform. Polym.* **2007**, *19*, 621.
31. Cho, T. K.; Chong, M. H.; Chun, B. C.; Kim, H. R.; Chung, Y. C. *Fiber Polym.* **2007**, *8*, 7.
32. DeSimone, J. M. *Science* **2002**, *297*, 799.
33. Poliakoff, M.; Fitzpatrick, J. M.; Farren, T. R.; Anastas, P. T. *Science* **2002**, *297*, 807.
34. Beckman, E. J. *Environ. Sci. Technol.* **2002**, *36*, 347A.
35. Heijkants, R. G. J. C.; Van Calck, R. V.; Van Tienen, T. G.; De Groot, J. H.; Buma, P.; Pennings, A. J.; Veth, R. P. H.; Schouten, A. J. *Biomaterials* **2005**, *26*, 4219.
36. Ping, P.; Wang, W.; Chen, X.; Jing, X. *J. Polym. Sci. Part B: Polym. Phys.* **2007**, *45*, 557.
37. Bil, M.; Ryszkowska, J.; Woźniak, P.; Kurzydłowski, K. J.; Lewandowska-Szumieł, M. *Acta Biomater.* **2010**, *6*, 2501.
38. Nečas, D.; Klapetek, P. *Cent. Eur. J. Phys.* **2012**, *10*, 181.
39. Yılgör, E.; Burgaz, E.; Yurtsever, E.; Yilgör, I. *Polymer* **2000**, *41*, 849.
40. Queiroz, D. P.; De Pinho, M. N.; Dias, C. *Macromolecules* **2003**, *36*, 4195.
41. Romanova, V.; Begishev, V.; Karmanov, V.; Kondyurin, A.; Maitz, M. F. *J. Raman Spectrosc.* **2002**, *33*, 769.
42. Liu, J.; Ma, D. *J. Appl. Polym. Sci.* **2002**, *84*, 2206.
43. Ewing, G. E. *J. Phys. Chem.* **1986**, *90*, 1790.
44. Yang, B.; Huang, W. M.; Li, C.; Li, L. *Polymer* **2006**, *47*, 1348.
45. Velayutham, T. S.; Abd Majid, W. H.; Gan, W. C.; Khorsand Zak, A.; Gan, S. N. *J. Appl. Phys.* **2012**, *112*, 054106.
46. Eceiza, A.; Larranaga, M.; De la Caba, K.; Kortaberria, G.; Marieta, C.; Corcuera, M. A.; Mondragon, I. *J. Appl. Polym. Sci.* **2008**, *108*, 3092.
47. Sarasam, A. R.; Krishnaswamy, R. K.; Madihally, S. V. *Biomacromolecules* **2006**, *7*, 1131.
48. Król, P.; Lechowicz, J. B.; Król, B. *Colloid Polym. Sci.* **2013**, *291*, 1031.